Electrical Properties of Niobium-Doped Titanium Dioxide. 2. Equilibration Kinetics†

L. R. Sheppard, T. Bak, and J. Nowotny*

Centre for Materials Research in Energy Conversion, School of Materials Science and Engineering, The University of New South Wales, Sydney, NSW 2052, Australia

Received: June 14, 2006; In Final Form: August 28, 2006

The present work reports isothermal gas/solid equilibration kinetics for Nb-doped TiO_2 (0.65 atom %) at elevated temperatures (1073−1298 K) within narrow ranges of oxygen activity spanning between 10^{-13} Pa and 75 kPa. The equilibration kinetics were monitored using electrical conductivity measurements. The kinetic data were used to determine the chemical diffusion coefficient (D_{chem}). D_{chem} as a function of $p(O_2)$ exhibits a complex dependence, which is considered in terms of defect disorder and the related concentrations of electronic charge carriers. The activation energy of D_{chem} in the $p(O_2)$ range 10 Pa < $p(O_2)$ < 75 kPa varies in the range 88.0−98.2 kJ/mol. It is important to note that the chemical diffusion coefficient in strongly reduced conditions [$p(O_2) = 10^{-9}$ Pa] exhibits a negative temperature dependence of D_{chem} (−67.2 kJ/mol). This finding indicates that under these conditions transport in a chemical potential gradient is consistent with metallic charge transport.

1. Introduction

The properties of nonstoichiometric oxides are determined by their defect disorder.[1,2] Therefore, these properties may be modified by changing the nonstoichiometry and the associated defect disorder. These may be achieved by the imposition of controlled oxygen activity at elevated temperatures. It is clear that well-defined defect disorder may be achieved when solid specimens reach equilibrium with the surrounding gas phase.

The defect disorder also may be modified by incorporating aliovalent ions, which form donors and acceptors. However, the incorporation mechanism of aliovalent ions depends on the oxygen activity, $p(O_2)$.[1−3] Thus, the imposition of a well-defined $p(O_2)$ over doped specimens is again required to achieve well-defined defect disorder.

The objective of the present study is to examine the effect of Nb on semiconducting properties of TiO_2 and the related defect disorder. The study is part of a research program aiming at the development of TiO_2-based oxide systems with enhanced photoelectrochemical properties through the imposition of controlled defect disorder. Part 1 of the present study reported the electrical properties of niobium-doped titanium dioxide (Nb−TiO_2), including the electrical conductivity and thermoelectric power.[3] These data were assessed in terms of the effect of oxygen activity, $p(O_2)$, on the defect disorder of Nb-doped TiO_2.

The processing of metal oxides at elevated temperatures with controlled defect disorder requires knowledge of the chemical diffusion coefficient (D_{chem}) in order to ensure that a gas/solid equilibrium is reached and defects are homogeneously distributed within the oxide specimen. Only then can the studied specimen be considered as well-defined. Therefore, the present work ultimately aims at the determination of chemical diffusion data for Nb-doped TiO_2.

Well-defined oxygen activity, $p(O_2)$, in the lattice may be achieved after the imposition of controlled $p(O_2)$ in the gas phase and its subsequent propagation into the bulk of the specimen. Therefore, knowledge of the gas/solid equilibration kinetics (or propagation kinetics) is essential for the selection of processing conditions, such as time and temperature, that are required for the uniform distribution of $p(O_2)$ within the lattice.

The imposition of a new $p(O_2)$ at the gas/solid interface of an oxygen/metal oxide system results in the establishment of a new $p(O_2)$ gradient and consequent propagation of a new $p(O_2)$ into the bulk, which leads to the annihilation of this concentration gradient. The process of propagation, which is described by D_{chem},[4−6] is controlled by the transport of defects under the influence of a chemical potential gradient. For metal oxides that exhibit low degrees of nonstoichiometry and weak interactions between defects, such as NiO, D_{chem} is independent of $p(O_2)$.[7] However, for oxides with high degrees of nonstoichiometry, such as TiO_2, D_{chem} exhibits a complex dependence on $p(O_2)$.[8] This complexity explains the presence of conflicting reports in the literature for the D_{chem} of TiO_2.[9−15]

It has been indicated previously[8] that most of the chemical diffusion data for TiO_2 reported so far are of limited applicability because either the studied specimens were not well-defined (in terms of the impurities) or the applied processing procedures were not well-defined (evidence of the gas/solid equilibrium was not provided). Consequently, these data reflect extrinsic properties rather than intrinsic properties of TiO_2.[8]

The present work is part of a research program that aims to determine the effect of niobium on the semiconducting and electrochemical properties of TiO_2. Niobium is of interest because it has a large solubility in TiO_2, which allows its properties to be modified over a wide range.[12] The preceding paper in this series reported the effects of niobium on the electrical conductivity (σ) and thermoelectric power (S).[3] The present study aims to determine D_{chem} for Nb-doped TiO_2 in order to assess the effect of Nb on the equilibration kinetics.

2. Definition of Terms

2.1. Mechanism of Niobium Incorporation. TiO_2 is a nonstoichiometric compound, more accurately considered to be either TiO_{2-x}, when exhibiting *n*-type properties, or TiO_{2+x}, for *p*-type material.[1,16] The defect disorder of undoped TiO_2

† The present work has been performed as part of an ongoing R&D program on solar hydrogen. The program aims at using titanium dioxide as a raw material for processing TiO_2-based oxide systems that are required to assemble high-performance photoelectrochemical cells for water splitting.

* Corresponding author. Phone: +61 2 9385 6465. Fax: +61 2 9385 6467. E-mail: J.Nowotny@unsw.edu.au.

10.1021/jp063703x CCC: $33.50
Published on Web 10/17/2006

generally is considered solely in terms of oxygen vacancies and titanium interstitials, which result in *n*-type semiconductivity.[1] However, it has been recently demonstrated that undoped TiO_2 may exhibit both *n*- and *p*-type properties,[16] where *p*-type properties are defined in terms of titanium vacancies, which are formed during the prolonged oxidation of TiO_2.

The mechanism of niobium incorporation into TiO_2 and the associated effect on the electrical properties depends on $p(O_2)$.[3,12,17] Under reducing conditions, the incorporation of niobium may be represented (using Kroger−Vink notation[18]), by the following reaction:

$$Nb_2O_5 \rightleftarrows 2Nb_{Ti}^{\bullet} + 2e' + 4O_O + \frac{1}{2}O_2 \quad (1)$$

In this case, the defect disorder is governed by electronic charge compensation:

$$n = [Nb_{Ti}^{\bullet}] \quad (2)$$

Consequently, the concentration of electrons and the resultant electrical properties are essentially independent of $p(O_2)$.

The incorporation of niobium into the lattice of TiO_2 under oxidizing conditions may be represented by the following reaction:

$$2Nb_2O_5 \rightleftarrows 4Nb_{Ti}^{\bullet} + V_{Ti}'''' + 10O_O \quad (3)$$

In this case, the defect disorder is governed by ionic charge compensation:

$$4[V_{Ti}''''] = [Nb_{Ti}^{\bullet}] \quad (4)$$

Consequently, the concentration of electronic charge carriers is the following function of $p(O_2)$:

$$n = K_i\left(\frac{[Nb_{Ti}^{\bullet}]}{4K_V}\right)^{1/4} p(O_2)^{-1/4} \quad (5)$$

where K_i is the intrinsic electronic equilibrium constant and K_V is the equilibrium constant for the following reaction:

$$O_2 \rightleftarrows V_{Ti}'''' + 2O_O + 4h^{\bullet} \quad (6)$$

It should be emphasized that, according to eqs 1−6, the mechanism of niobium incorporation into TiO_2 is determined by the $p(O_2)$ in the lattice and not the $p(O_2)$ in the gas phase; the difference between the two may be substantial, when gas/solid equilibrium is not achieved. Therefore, knowledge of the gas/solid equilibration kinetics is an essential precondition for the correct assessment of data describing the relevant electrical properties, including electrical conductivity, σ, and thermoelectric power, *S*.

2.2. Gas/Solid Kinetics. Equilibrium in an oxygen/metal oxide system and the associated nonstoichiometry are determined by the $p(O_2)$ in the gas phase and the temperature. At a gas/solid equilibrium, the concentration of defects is well-defined by these conditions. When either the $p(O_2)$ or temperature is changed for an initially equilibrated homogeneous oxide crystal, the system responds by tending toward and ultimately achieving a new equilibrium state and associated nonstoichiometry. A new concentration of defects is imposed at the surface almost immediately, and this is propagated into the bulk phase in order to attain a new chemical potential for oxygen throughout the crystal. The rate of the propagation of these defects is determined by chemical diffusion.[4−6]

The determination of well-defined chemical diffusion data requires the following issues to be addressed:

(i) The generation of well-defined data for the equilibration kinetics is required. This is the case when the system is in equilibrium both before and after the equilibration process. Thus, the kinetics data may be considered to be well-defined only when there is evidence that a gas/solid equilibrium has been achieved.

(ii) D_{chem} must be determined from equilibration kinetics data within narrow ranges of oxygen activity because the properties of nonstoichiometric compounds, including D_{chem}, may vary with nonstoichiometry. This applies to TiO_2, of which nonstoichiometry is very high.

(iii) D_{chem} must reflect bulk lattice diffusion under a chemical potential gradient and be independent of surface effects. Therefore, it is essential to know whether the effect of the surface on the gas/solid kinetics may be ignored.

D_{chem} may be determined using the relevant solution of the diffusion equation proposed by Crank:[19]

$$\gamma = 1 - \prod_{m=1}^{m=3}\left[\sum_{n=1}^{\infty}\frac{2L_m^{\,2}\exp\left(\frac{-\beta_n^{\,2}D_{chem}t}{l_m^{\,2}}\right)}{\beta_n^{\,2}(\beta_n + L_m^{\,2} + L_m)}\right] \quad (7)$$

where γ is the degree of equilibration [defined as $\gamma = \Delta\sigma_t/\Delta\sigma_\infty$, where $\Delta\sigma_t$ is the change in electrical conductivity after time *t* and $\Delta\sigma_\infty$ is the change in electrical conductivity after the achievement of the new equilibrium state, both relative to $t = 0$ when the new $p(O_2)$ is applied to the surface], L_m is a kinetics parameter (defined as $L_m = l_m k'/D_{chem}$), where l_1, l_2, and l_3 are the half-thicknesses of the specimen dimensions, k' is the rate constant of the surface reaction, and β_n are positive roots of the equation $L_m = \beta \tan \beta$. When the predominant defects in TiO_2 are oxygen vacancies, the degree of equilibration (γ) may be defined as

$$\gamma = \frac{[V_O^{\bullet\bullet}]_t - [V_O^{\bullet\bullet}]_0}{[V_O^{\bullet\bullet}]_\infty - [V_O^{\bullet\bullet}]_0} = \frac{\Delta\sigma_t}{\Delta\sigma_\infty} \quad (8)$$

where the subscripts *t*, 0, and ∞ denote some time, the initial stage, and the final stage, respectively.

It has been shown that the defect disorder of TiO_2 is complex, and it includes oxygen vacancies,[1] titanium interstitials,[1] and titanium vacancies.[16] However, the gas/solid kinetics may be considered in terms of oxygen vacancies only, as expressed by eq 8, because of the following reasons:

(i) Under the conditions of $p(O_2)$ used in the present work, the predominant mobile ionic defects are oxygen vacancies.[1]

(ii) Titanium interstitials are the minority defects, so their mass transport in the overall gas/solid process can be ignored.[1]

(iii) The diffusion rate of titanium vacancies is several orders of magnitude lower than that of oxygen vacancies. Therefore, it is reasonable to assume that these defects are immobile and so their concentration in the experimental conditions generally applied for testing electrical properties remains essentially unchanged.[16]

The effect of $p(O_2)$ on D_{chem}, and the associated nonstoichiometry of metal oxides, may be considered using the relation derived on the basis of the considerations of Wagner:[20−22]

$$D_{\text{chem}} = -\frac{kT\sigma_i t_{\text{el}}}{16e^2}F^{-1} \tag{9}$$

where k is Boltzmann's constant, T is the absolute temperature, σ_i is the electrical conductivity component arising from ions, t_{el} is the transference number of electronic charge carriers, e is the elementary charge, and F is[22]

$$F = \frac{\partial[V_{\text{O}}^{\bullet\bullet}]}{\partial \ln p(\text{O}_2)} = -\frac{1}{8}(n+p) \tag{10}$$

The expression for D_{chem}, represented by eq 9, may be expressed in a form that includes the concentrations of electronic charge carriers in the forms of electrons (n) and electron holes (p):[22]

$$D_{\text{chem}} = \frac{kT\sigma_i t_{\text{el}}}{2e^2}\frac{1}{n+p} \tag{11}$$

Equation 11 is particularly useful for the assessment of amphoteric semiconductors, such as TiO_2.

3. Experimental Section

The relevant data for the polycrystalline specimen of Nb-doped TiO_2 including the powder fabrication, processing procedures, structure, and microstructure are described elsewhere.[3] The total concentrations of acceptor-type cation impurities and anions (Cl) were 33.9 and 20 ppm, respectively. The size of the rectangular specimen was 1.74 mm × 3.80 mm × 14.91 mm. The average grain size was 5−10 μm. Details of the equipment for monitoring the electrical properties also is described elsewhere.[23,24]

The equilibration kinetics were determined for two $p(O_2)$ regimes, including the following:

(i) The first regime is the high-$p(O_2)$ regime. The $p(O_2)$ in this regime was imposed by an argon/oxygen mixture in the range 10 Pa to 75 kPa (gas flow rate of 100 mL/min).

(ii) The second regime is the low-$p(O_2)$ regime. The $p(O_2)$ in this regime was imposed by a hydrogen/argon/water vapor mixture in the range 10^{-13} to 10^{-5} Pa (gas flow rate of 100 mL/min). This $p(O_2)$ was achieved by passing a 1:99 hydrogen/argon mixture (diluted in argon), through a bubbler with deionized water kept at a constant temperature.

The oxygen activities in the high- and low-$p(O_2)$ regimes do not overlap because of the experimental limitations. The applied argon/oxygen and hydrogen/water vapor mixtures did not allow to obtain gas compositions with oxygen activities in the intermediate range. The gap between these two regimes is approximately 5 orders of magnitude.

The experimental $p(O_2)$ was determined using a zirconia-based electrochemical oxygen probe. The experiments in which the $p(O_2)$ was increased or decreased are termed oxidation or reduction experiments, respectively. The equilibration kinetics were determined for both oxidation and reduction runs at six temperatures: 1073, 1198, 1223, 1248, 1273, and 1298 K. The temperature was monitored during the equilibration runs. The consistency of the data was checked for repeatability.

Figure 1 shows the experimental monitoring sheet during a single oxidation experiment at 1273 K. The monitored quantities included oxygen activity [$p(O_2)$], temperature (T), and electrical conductivity (σ). As seen in the middle part of Figure 1, the temperature remained essentially constant with a fluctuation of ±0.5 K. It can be seen in the lowest part of Figure 1 that the electrical conductivity reaches a constant value within 1 h, although the electrical conductivity was monitored for at least

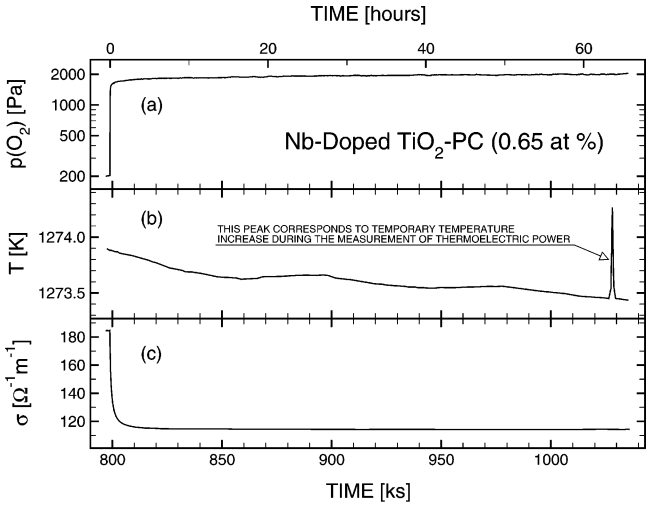

Figure 1. Standard monitoring sheet at 1273 K showing (a) changes in oxygen activity [$p(O_2)$], (b) the average of two temperature (T) measurements at both ends of the specimen, and (c) electrical conductivity (σ) determined from two resistance values taken at the same current but flowing in two different directions.

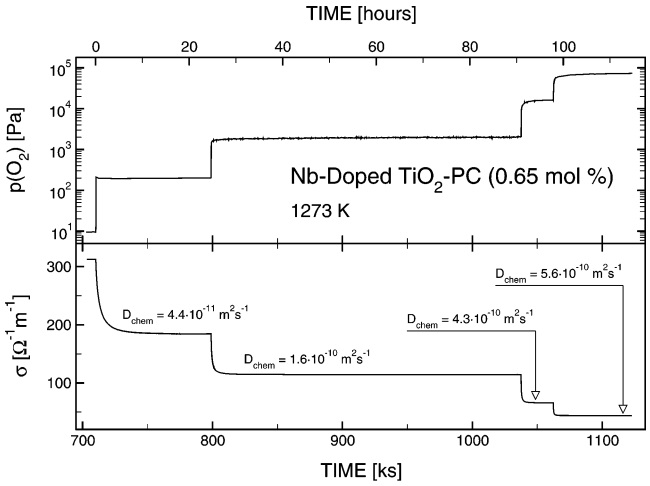

Figure 2. Kinetics of sequential oxidation at 1273 K showing (a) stepwise changes in oxygen activity [$p(O_2)$] and (b) associated changes in the electrical conductivity (σ).

20 h. The electrical conductivity exhibits such stability during both oxidation and reduction runs. The data reached 99.9% of the final electrical conductivity within 2 and 0.5 h at 1073 and 1298 K, respectively. The details of the experimental procedure are reported elsewhere.[24]

Figure 2 shows the stepwise changes in oxygen activity [$p(O_2)$] and electrical conductivity (σ) as a function of time within successive oxidation experiments. These kinetic data were used to determine the D_{chem} for each run within narrow ranges of $p(O_2)$. The determined data were then plotted as a function of $p(O_2)$.

4. Results and Discussion

4.1. Effect of Oxygen Activity. The chemical diffusion coefficient was determined using a computer program that allows minimization of the following error function:

$$\text{err} = \sum(\sigma_{\text{exp}} - \sigma_{\text{theor}})^2 \tag{12}$$

where err is the error function, σ_{exp} denotes the experimental data of the electrical conductivity during oxidation/reduction, and σ_{theor} is the theoretical value derived by the diffusion

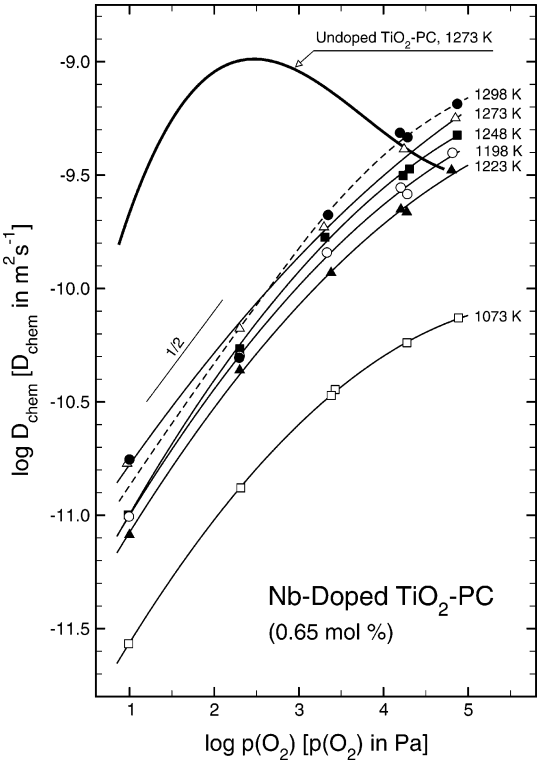

Figure 3. Chemical diffusion coefficient (D_{chem}) for polycrystalline Nb-doped TiO_2 in the range 1073−1298 K along with data for polycrystalline undoped TiO_2 at 1273 K as a function of $p(O_2)$ determined during (reproducible) oxidation and reduction runs in the high-$p(O_2)$ range (~10 Pa to 75 kPa).

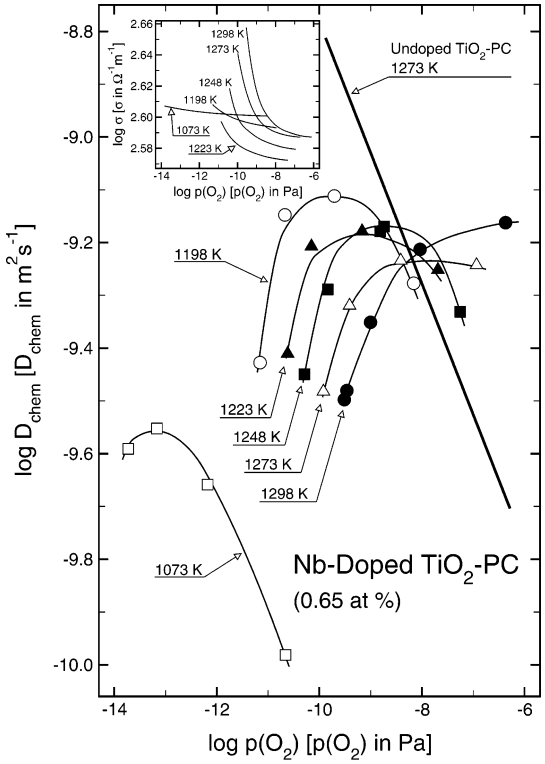

Figure 4. Chemical diffusion coefficient (D_{chem}) for polycrystalline Nb-doped TiO_2 in the range 1073−1298 K along with data for polycrystalline undoped TiO_2 at 1273 K as a function of $p(O_2)$ determined during (reproducible) oxidation and reduction runs in the low-$p(O_2)$ range (~10^{-14} to 10^{-7} Pa).

equation, eq 7. In the first attempt, the program adjusted the parameters of eq 7, involving D_{chem}, the rate constant k', and the final conductivity value, σ_∞, to achieve a minimum of err expressed by eq 12. This procedure indicated that the expression $l_m k'$ (for the smallest l_m) is 17 orders of magnitude larger than D_{chem}. Therefore, it is concluded that the gas/solid kinetics are determined by bulk diffusion and not surface reaction. Consequently, D_{chem} was determined assuming that bulk diffusion is rate-controlling the gas/solid equilibration. The stopping criterion of this iterative procedure was err $< 10^{-5}$.

Figures 3 and 4 show a typical scatter of the experimental data for high- and low-$p(O_2)$ ranges, respectively, and reference data for undoped TiO_2. It can be seen that the consistency of the data for individual temperatures is good and that the reproducibility for successive runs, as shown by the approximately vertical pairs of data points, is also good. Figure 5 combines the data from Figures 3 and 4 and shows the effects of $p(O_2)$ on D_{chem} for the complete ranges of temperature and $p(O_2)$ studied in the present work. Figure 5 is discussed subsequently.

4.1.1. High-p(O2) Regime. While polycrystalline undoped TiO_2 in the high-$p(O_2)$ regime exhibits an $n-p$ transition, the incorporation of 0.65 atom % niobium leads to the imposition of *n*-type conduction over the entire $p(O_2)$ range studied.[3] Figure 3 shows that undoped TiO_2 exhibits a maximum in D_{chem} at a $p(O_2)$ of ~320 Pa, which corresponds to the $n-p$ transition determined from the σ and S data. This is in agreement with eq 11. Similar maxima are expected for Nb-doped TiO_2, although at substantially higher $p(O_2)$ levels.

The data for Nb-doped TiO_2 exhibit the following characteristic features:

(i) Increasing the $p(O_2)$ results in an increase in the D_{chem} by approximately 2 orders of magnitude. The effect of $p(O_2)$ on D_{chem} in this $p(O_2)$ regime is substantially larger than that for undoped TiO_2.

(ii) The increasing nature of the log D_{chem} versus log $p(O_2)$ dependence suggests the existence of maxima at $p(O_2)$ levels larger than 75 kPa. This tendency is clearest at the lowest temperature of 1073 K.

(iii) The D_{chem} data exhibit good consistency and reproducibility for different temperatures and successive oxidation/reduction runs.

The observed effect of the strong increase in D_{chem} with increasing $p(O_2)$ for Nb-doped TiO_2 is consistent with a similar effect observed for polycrystalline undoped TiO_2 in the *n*-type regime.[25] It is clear that the incorporation of niobium results in a shift of the $n-p$ transition points toward higher $p(O_2)$ levels that are beyond the $p(O_2)$ range used in this work. Consequently, eq 11 indicates that the D_{chem} for Nb-doped TiO_2 is expected to reach maxima at the $p(O_2)$ levels that are substantially higher than atmospheric pressure.

The observed effect of $p(O_2)$ on D_{chem} may be described by the following empirical expression:

$$D_{chem} = D^0_{chem}\, p(O_2)^{1/n} \tag{13}$$

where D^0_{chem} is the D_{chem} in the standard state and the $p(O_2)$ exponent, $1/n$, is the slope of the log D_{chem} versus log $p(O_2)$ dependence. It can be seen in Figure 3 that the $p(O_2)$ exponent for undoped TiO_2 in the *n*-type regime (left of the maximum in D_{chem}) is similar to those for Nb-doped TiO_2 ($1/n = \sim 1/2$).

4.1.2. Low-p(O2) Regime. Figure 4 shows that the effect of low-$p(O_2)$ levels on D_{chem} is more complex than that of high-$p(O_2)$ levels. The character of the changes in D_{chem} versus $p(O_2)$ depends on the established conduction mechanism.[3] In the temperature range 1198−1298 K, the D_{chem} levels increase with

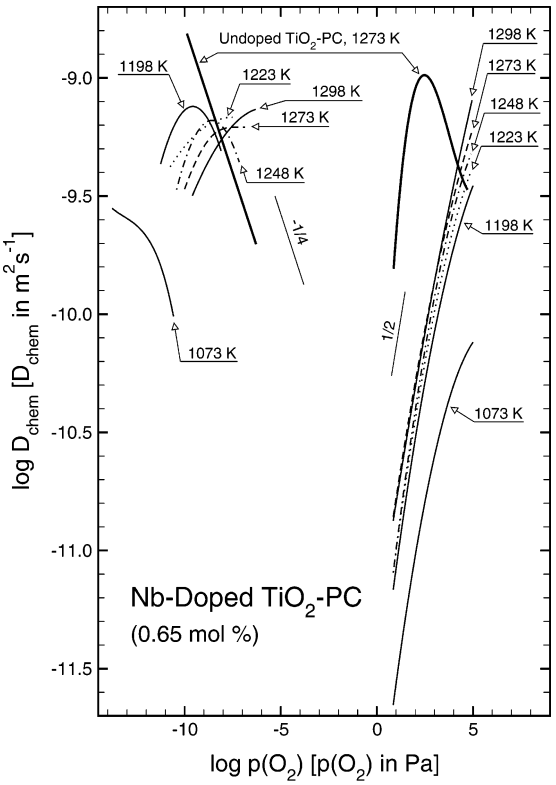

Figure 5. Collection of all data of the chemical diffusion coefficient (D_{chem}) for polycrystalline Nb-doped TiO_2 in the range 1073−1298 K along with data for polycrystalline undoped TiO_2 at 1273 K as a function of $p(O_2)$ determined during (reproducible) oxidation and reduction runs in the entire $p(O_2)$ range ($\sim 10^{-14}$ Pa to 75 kPa).

increasing $p(O_2)$ by less than half of an order of magnitude, and they have a tendency to reach maxima, which are observed clearly at 1198, 1223, and 1248 K. However, the character of the change in D_{chem} is entirely different at 1073 K, where D_{chem} initially increases only slightly, with a stronger tendency to decrease with increasing $p(O_2)$. The data for polycrystalline undoped TiO_2 show a consistent linear decreasing trend with increasing $p(O_2)$.[25]

It should be noted that this low-$p(O_2)$ regime exhibits exceptional electronic properties, which overlap two types of defect disorders where the electrical properties are related to the following charge compensation mechanisms:

(i) Positively charged niobium ions are incorporated in the titanium lattice sites and they are compensated by electrons (*n*-type):

$$[Nb_{Ti}^{\bullet}] = n \tag{14}$$

This regime is predominant in the lower temperature range (1073−1248 K). It is attributed to quasimetallic charge transport,[3] and this state corresponds to the presence of maxima in the data.

(ii) With increasing temperatures, the system increasingly involves positively charged oxygen vacancies as the predominant defects, which are compensated by electrons (*n*-type):

$$2[V_O^{\bullet\bullet}] = n \tag{15}$$

This charge compensation, which corresponds to the strongly reduced regime, applies at the highest temperature range (1273−1298 K). This regime is consistent with semiconducting charge transport,[3] and this state corresponds to the absence of maxima in the data.

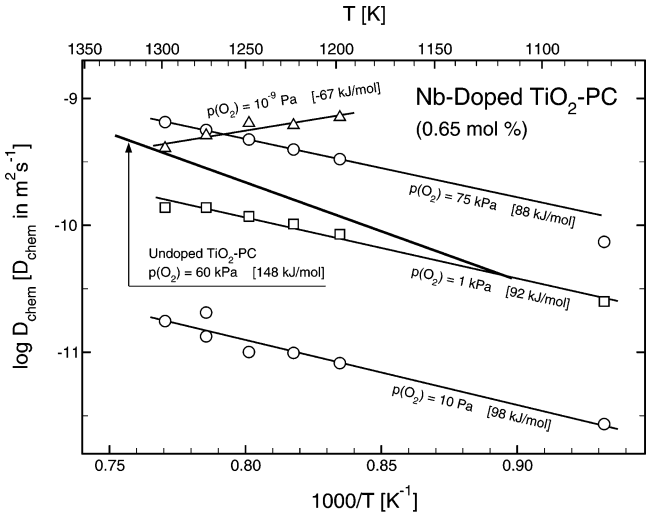

Figure 6. Arrhenius plots of the chemical diffusion coefficient (D_{chem}) for Nb-doped TiO_2 determined within narrow $p(O_2)$ ranges (final levels of 10^{-9} Pa, 10 Pa, 1 kPa, and 75 kPa).

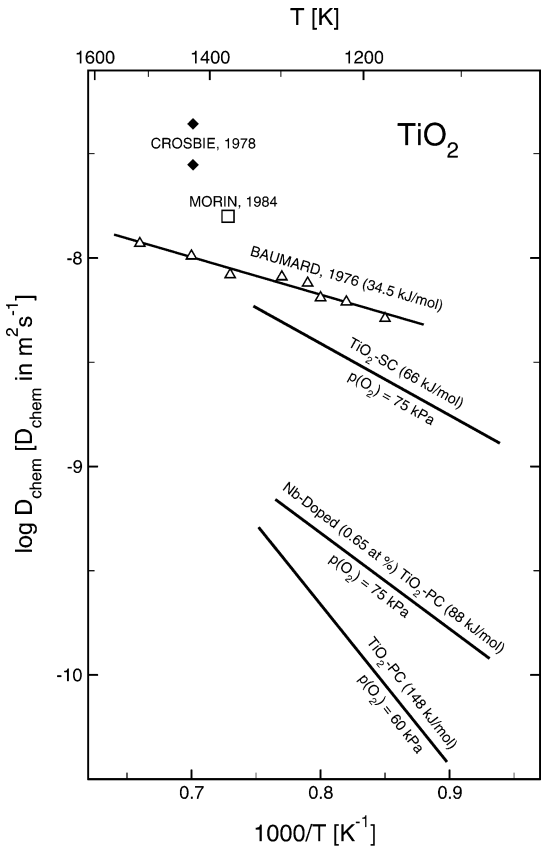

Figure 7. Arrhenius plots of the chemical diffusion coefficient (D_{chem}) for Nb-doped TiO_2 compared to the literature data in the high-$p(O_2)$ range.

It is essential to be aware that the concentration of oxygen vacancies in strongly reduced TiO_2 in the low-$p(O_2)$ regime assumes very high values.[26] This results in strong interactions between defects, thereby leading to the formation of shear structures[1,2] and larger defect aggregates.[27] Consequently, the observed complex dependence between D_{chem} and $p(O_2)$ in this regime is a reflection of several concurrent effects.

As seen in Figure 5, there is a gap between these two sets of data (corresponding to low and high oxygen-activity regimes), which is due to the experimental limitations.

4.2. Effect of Temperature. Because D_{chem} varies with $p(O_2)$, the effect of temperature on D_{chem} should be considered within

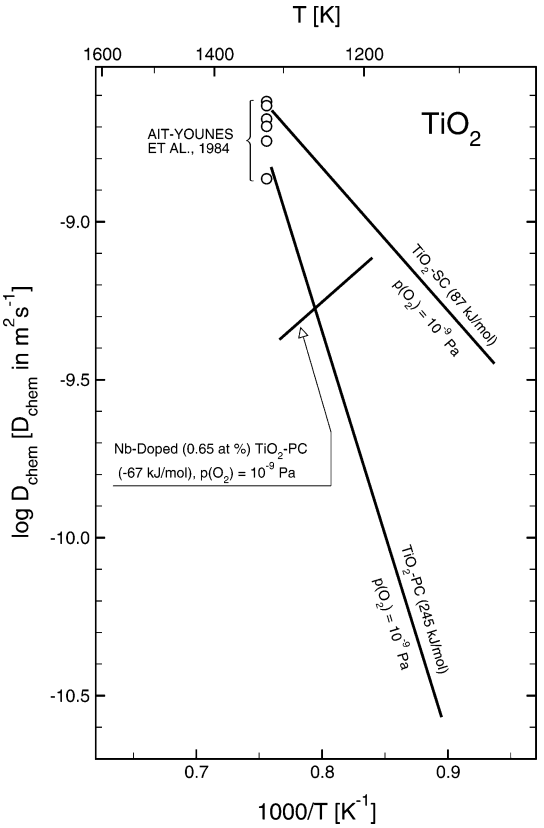

Figure 8. Arrhenius plots of the chemical diffusion coefficient (D_{chem}) for Nb-doped TiO_2 compared to the literature data in the low-$p(O_2)$ range.

relatively narrow ranges of $p(O_2)$. Figure 6 shows isobaric Arrhenius plots of D_{chem} determined at several final $p(O_2)$ values. As seen, the activation energy of D_{chem} at $p(O_2) \geq 10$ Pa remains in the range 88−98 kJ/mol. However, at $p(O_2) = 10^{-9}$ Pa, the positive slope of the data indicates that the chemical diffusion is not an activated process. Over this temperature range (∼1200−1300 K), the temperature coefficient of D_{chem} is −67 kJ/mol, which demonstrates that the mechanism of the transport of defects under a chemical potential gradient is exceptional. In this regime, the metallic conductivity mechanism has been established.[3] Consequently, it may be considered that this exceptional behavior is characteristic of metallic conductivity.

The D_{chem} data for Nb-doped TiO_2 are compared to D_{chem} values for undoped TiO_2 in Figures 7 and 8 at high and low $p(O_2)$, respectively.

4.2.1. High Oxygen Activity. Isobaric plots of log D_{chem} versus $1/T$ for Nb-doped $p(O_2)$ at high $p(O_2)$ levels are shown in Figure 7. This figure also shows the data for undoped TiO_2, including polycrystalline TiO_2 [25] and single crystals,[28] obtained using an identical procedure and the same equipment, as well as data reported by Baumard,[12] Crosbie,[13] and Morin[15] determined in similar conditions. As seen, the absolute values of D_{chem} for Nb-doped TiO_2 are substantially lower than those for TiO_2 single crystals. However, the data of D_{chem} for Nb-doped TiO_2 and undoped polycrystalline TiO_2 are comparable, while the activation energy for the undoped polycrystalline specimen is the highest one.

4.2.2. Low Oxygen Activity. Isobaric plots of log D_{chem} versus $1/T$ for Nb-doped TiO_2 at low $p(O_2)$, along with the data reported by Ait-Younes et al.,[14] are shown in Figure 8. As seen, D_{chem} for Nb-doped TiO_2 exhibits a negative temperature coefficient, while the undoped TiO_2 specimens, both polycrystalline and single-crystal, show positive activation energies.

The negative value of the temperature coefficient of D_{chem} established in the present work, which is shown in Figure 8, is the first ever observed effect of this kind for metal oxides in general and TiO_2 in particular. This effect is observed under conditions close to those in which the Nb−TiO_2 specimen exhibits metallic-type conductivity. This effect may be considered in terms of ambipolar diffusion under a chemical potential gradient. Specifically, the chemical diffusion involves the transport of both ionic and electronic species, where usually faster electronic defects result in an enhancement of the transport of ionic defects. Because in the metallic state the mobility of electronic charge carriers decreases with increasing temperature (because of increased interactions with phonons), the negative value of the temperature coefficient of D_{chem} indicates that the electronic conductivity component plays an important role in chemical diffusion for Nb-doped TiO_2 in reduced conditions.

5. Conclusions

The observed dependence of D_{chem} as a function of $p(O_2)$ for polycrystalline Nb-doped TiO_2 is a reflection of the complex defect disorder and its impact on the transport kinetics under a chemical potential gradient.

The strong increase in D_{chem} as a function of $p(O_2)$ for polycrystalline Nb-doped TiO_2 in the high-$p(O_2)$ regime is consistent with the similar dependence observed for polycrystalline undoped TiO_2 in the high-$p(O_2)$ regime. However, the observed changes in D_{chem} in this regime are substantially higher for the doped specimen. The activation energy of D_{chem} in this regime is in the range 88−98 kJ/mol.

The observed complex dependence between D_{chem} and $p(O_2)$ in the low-$p(O_2)$ regime can be interpreted in terms of an overlap of electronic and ionic charge compensations. Strong interactions between the defects, leading to the formation of shear structures and defect aggregates, can be expected to have an effect on the transport in this regime. The negative value of the temperature dependence of D_{chem} confirms the unusual transport mechanisms in this regime.

Acknowledgment. The present work was supported by the Australian Research Council, Rio Tinto Ltd., Brickworks Ltd., Mailmasters Pty. Ltd., Sialon Ceramics Pty. Ltd., and Avtronics (Australia) Pty. Ltd. The support of the Australian Institute of Nuclear Science and Engineering (AINSTU1003) also is gratefully acknowledged.

References and Notes

(1) Kofstad, P. *Nonstoichiometry, Diffusion and Electrical Conductivity in Binary Metal Oxides*; Wiley: New York, 1972.
(2) Matzke, Hj. In *Nonstoichiometric Oxides*; Sorensen, O. T., Ed.; Academic Press: New York, 1981.
(3) Sheppard, L. R.; Bak, T.; Nowotny, J. *J. Phys. Chem. B* **2006**, *110*, 22447.
(4) Chils, P. E.; Wagner, J. B., Jr. In *Heterogeneous Kintics at Elevated Temperatures*; Bolton, G. R., Worrell, W. L., Eds.; Plenum Press: New York, 1970; p 269.
(5) Levin, R. L.; Wagner, J. B., Jr. *Trans. Metall. Soc. AIME* **1965**, *233*, 159.
(6) Price, J. B.; Wagner J. B., Jr. *Z. Physik. Chem., Neue Folge* **1966**, *49*, 257.
(7) Nowotny, J.; Sadowski, A. *J. Am. Ceram. Soc.* **1979**, *62*, 24.
(8) Nowotny, J.; Bak, T.; Nowotny, M. K.; Sorrell, C. C. *Phys. Status Solidi B* **2005**, *242*, R91.
(9) Barbanel, V. I.; Bogomolov, V. N. *Sov. Phys. Solid State* **1970**, *11*, 2160.
(10) Moser J.; Childs, P. E.; Wagner J. B., Jr. *Proc. Br. Ceram. Trans.* **1971**, *19*, 29.
(11) Iguchi, E.; Yajima, K. *J. Phys. Soc. Jpn.* **1972**, *32*, 1415.
(12) Baumard, F. *Solid State Commun.* **1976**, *20*, 859.
(13) Crosbie, G. M. *J. Solid State Chem.* **1978**, *25*, 367.

(14) Ait-Younes, A.; Millot, F.; Gerdanian, P. *Solid State Ionics* **1984**, *12*, 437.
(15) Morin, F. *Solid State Commun.* **1986**, *58*, 161.
(16) Nowotny, M. K.; Bak, T.; Nowotny, J.; Sorrell, C. C. *Phys. Status Solidi B* **2005**, *242*, R88.
(17) Baumard, F.; Tani, E. *Phys. Status Solidi* **1977**, *39*, 373.
(18) Kroger, F. A. *The Chemistry of Imperfect Crystals*; North-Holland: Amsterdam, 1974; Vol. 3.
(19) Crank, J. *The Mathematics of Diffusion*, 2nd ed.; Oxford University Press: Oxford, U. K., 1975.
(20) Wagner, C. *Z. Phys. Chem., Abt. B* **1933**, *B21*, 25.
(21) Wagner, C. *Prog. Solid State Chem.* **1975**, *10*, 3.
(22) Grzesik, Z.; Bak, T.; Nowotny, J. *Adv. Appl. Ceram.* Submitted.
(23) Nowotny, J. In *The CRC Handbook of Solid-State Electrochemistry*; Gellings, P. J., Bouwmeester, H. J. M., Eds.; CRC Press: Boca Raton, FL, 1997; pp 131−159.
(24) Bak, T.; Nowotny, J.; Sorrell, C. C.; Zhou, M. F. *J. Mater. Sci.: Mater. Electron.* **2004**, *15*, 635.
(25) Burg, T. Ph.D. Thesis, The University of New South Wales, School of Materials Science and Engineering, Sydney, Australia, in progress.
(26) Bak, T.; Nowotny, J.; Rekas, M.; Sorrell, C. C. *J. Phys. Chem. Solids* **2003**, *64*, 1057.
(27) Stoneham, M. *Phys. Today* **1980**, *33*, 34.
(28) Nowotny, M. K. Ph.D. Thesis, The University of New South Wales, School of Materials Science and Engineering, Sydney, Australia, in progress.